Weeding Manipulator Exploiting Its Oscillatory Motion for Force Generation: Verification of the Effectiveness by Simulations using Open Dynamics Engine

Jun Kobayashi

Department of Systems Design and Informatics
Kyushu Institute of Technology
Kawazu 680-4, Iizuka, Fukuoka, 820-8502, Japan

jkoba@ces.kyutech.ac.jp

Abstract – **This paper addresses a weeding manipulator exploiting its oscillatory motion to generate a large force efficiently. To justify the exploitation, some simulations were conducted based on a manipulator model and a weed model created using Open Dynamics Engine (ODE), which is a high performance library for simulating rigid body dynamics. The simulation results illustrated that the exploitation of an oscillatory motion is effective on force generation by a manipulator. Furthermore, it was shown that a manipulator drive method using Van der Pol (VDP) oscillator has better performance than a method using a sinusoidal wave function, because of an entrainment property of the VDP oscillator.**

Index Terms – *Weeding Manipulator, Force Generation, Oscillatory Motion, Van der Pol Oscillator, Open Dynamics Engine*

I. INTRODUCTION

Weeding is a necessary task to keep a house and a park beautiful, but you hate to be involved in such a task in general because it is boring. Therefore a robot would be able to make you happy if it can execute the task without human intervention. To realize a weeding robot working automatically, several technologies are needed: manipulation, image recognition, navigation, etc. This paper addresses large force generation of the weeding robot. The weeding robot is required to generate a large force, because some weeds have roots spreading deeply and tightly. Performance of the robot would be improved by providing powerful actuators, but such a robot would consume energy uselessly owing to the heavy weight of the powerful actuators.

Efficiency is essential factor for robots, especially for robots working outdoors driven by batteries. Inefficient robots would be useless because it cannot execute enough tasks within its uptime. Some studies have been conducted to realize efficient robots that exploit their characteristics to the maximum to achieve an efficient behavior. Papadopoulos and Gonthier have introduced the force workspace, which is a map indicating the locations where a robot can apply a given force [1]. With the workspace, they showed that force capabilities of manipulators can be improved by employing base mobility and manipulator redundancy. Imamura and Kosuge have proposed virtually unactuated joints so that a manipulator could generate a larger force than the load capacity [2]. Kobayashi, Kishida and Ohkawa have formulated an optimization problem and solved it to find out work postures in which a robot manipulator realizes a force as large as possible [3].

The author has studied a manipulator that can efficiently generate a large force in a way that the manipulator exploits its oscillatory motion [4][5]. Fig. 1 explains the idea of the way. The weeding manipulator has a plate spring as the end-effector and exploits its oscillation property attributed to the spring element. The manipulator is driven by the method proposed in the author's papers so that it can oscillate adequately, and then the manipulator in oscillatory motion applies an oscillatory force to a weed through the spring.

A manipulator model used in the previous study includes a constraint to make analyses simple, and the effectiveness of the exploitation of an oscillatory motion has been verified based on the simplified model. The manipulator model, however, is impractical for typical tasks. The manipulator can be used only for oscillatory force generation, but not for other tasks. Therefore, in this paper, a more practical model is created, and verification of the effectiveness of the exploitation is conducted using the new manipulator model.

This paper is organized as follows. The new models of the weeding manipulator and the weed are introduced in the section II. In the section III, a control scheme for the weeding
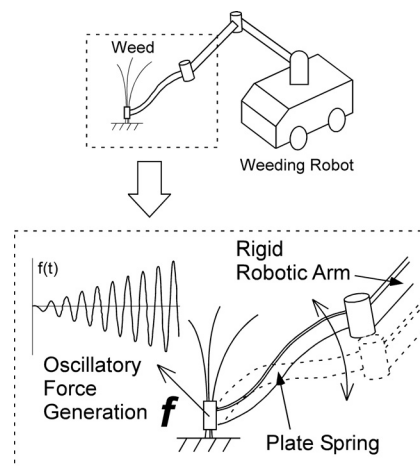

Fig. 1 Concept diagram. The weeding manipulator is equipped with a plate spring as the end-effector. The manipulator exploits its oscillatory motion, generating a large force efficiently.

manipulator is shown, and two methods to oscillate the manipulator exploiting its oscillatory motion for force generation are discussed. Simulation results that justify the exploitation are shown in the section IV. Finally, this paper is concluded in the section V.

II. SIMULATION MODEL

To show the effect of oscillatory motions of a manipulator on force generation, some simulations have been conducted based on the manipulator model shown in Fig. 2 [4][5]. As shown in this figure, the movement of the manipulator is constrained by a rail, the tip of the manipulator can move only along the rail. The constraint reduces the degree of freedom of the manipulator from two to one, and thereby the behavior of the manipulator has been able to be analyzed simply. This model, however, is impractical; the manipulator with the constraint can be used only for oscillatory force generation, but not for other tasks.

By the simulations conducted based on the simplified model, the effectiveness of oscillatory motions on force generation has been demonstrated. Therefore, in this paper, this study must go to the next step; the effectiveness should be confirmed using simulations based on the more practical manipulator model. In order to conduct such a simulation, Open Dynamics Engine (ODE) was used in all simulations described in this paper. The ODE is an open source, high performance library for simulating rigid body dynamics [6]. All simulations described in this paper are carried out based on a weeding manipulator model and a weed model created using rigid body objects of the ODE. Those models are explained in the following subsections.

A. Weeding Manipulator Model

The manipulator dealt with in this paper consists of four rigid links, four joints and a base. The model of the manipulator created on the simulation program using the ODE is shown in Fig. 3. It is assumed that the stiffness of each joint is variable; the joints have compliance that has been realized for a manipulator in several ways (e.g. [7][8]). In this model, as the manipulator is weeding, the third joint becomes a free joint, and the fourth joint becomes a spring joint, and thereby two distal links painted yellow work like a spring. This condition is feasible because the stiffness of the joints can be changed. When a typical task is assigned to the manipulator,
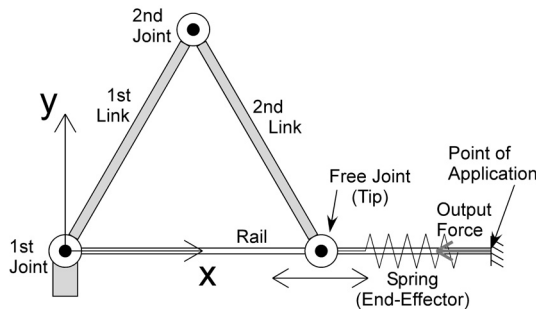

Fig. 2 Former model of a manipulator equipped with a spring as the end-effector. The manipulator applies an oscillatory force to a certain point through the spring.
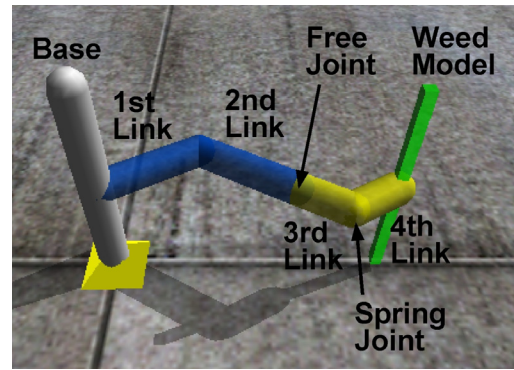

Fig. 3 Weeding manipulator model and weed model created using the ODE.

all four links are used ordinarily. If the typical task is a positioning of an object, the stiffness of the all four joints is set to rigid to achieve the task accurately. Unlike the impractical manipulator model shown in Fig. 2, the manipulator adopted in this paper in Fig. 3 is more practical because its structure is similar to a structure of a normal manipulator.

In the following, the position of the tip of the manipulator that is connected to the weed model is designated by symbols x_t and y_t, and the position of the third joint that is a boundary position between the distal links that work like a spring and the proximal links is designated by symbols x_{t2} and y_{t2}. The spring constant of the fourth joint is set to 1.0 Nm/rad. The other parameters of the manipulator are set as follows: the length and the mass of the first and second links are 0.1 m and 0.5 kg respectively, the length and the mass of the third and fourth links is 0.05 m and 0.25 kg respectively. The damping coefficient of the first and second joints is 0.1 Nms/rad. The torques driving the joints are limited to 1.0 Nm.

B. Weed Model

In the simulations using the ODE, a weed is modeled using a rectangular solid object. The green object shown in Fig. 3 is the weed model. When the weed model is moved from its base point, a restoring force is generated as shown in Fig. 4. The red arrow shown in Fig. 4 indicates the vector of the restoring force. The magnitude of the force vector depends on the displacement from the base point, which is designated by Δx in equations described later. The restoring force acts on the weed model and the direction of the force vector points toward the base point; the weed model is brought back to the base point by the restoring force. The restoring force modeled in this study is decomposed into an elastic force and a viscous force. Fig. 5 shows the characteristics of the magnitude of the elastic restoring force. In Fig. 5, d_{min} is a radius of the dead zone of the elastic restoring force, which is represented by the circular area in light blue in Fig. 4. The viscous restoring force acts even in the dead zone. The blue circle represents the effective range of the two restoring forces; out of the range the restoring forces do not have effect. The effective radius of the range is d_{max}. The weed displacement of more than d_{max} means that the manipulator has succeeded in pulling the weed out.
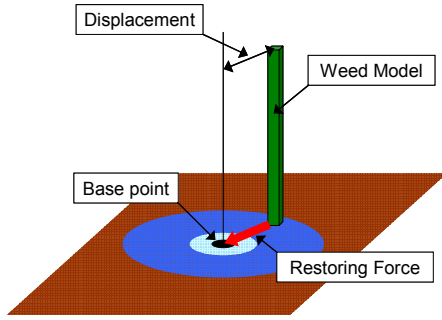
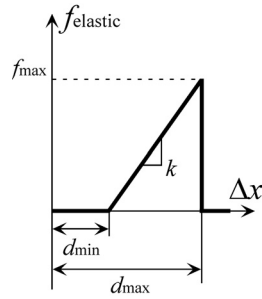Fig. 4 Schematic of the restoring force of the weed mode.

Fig. 5 Characteristic of the elastic restoring force.

Equation (1) and (2) describe the elastic and viscous restoring forces respectively.

$$f_{elastic} = \begin{cases} 0 & (\Delta x < d_{min}) \\ k \cdot (\Delta x - d_{min}) & (d_{min} \leq \Delta x \leq d_{max}) \\ 0 & (\Delta x > d_{max}) \end{cases} \quad (1)$$

$$f_{viscous} = \begin{cases} c \cdot d\Delta x/dt & (\Delta x \leq d_{max}) \\ 0 & (\Delta x > d_{max}) \end{cases} \quad (2)$$

The parameters of the weed model are set as follows: the mass of the weed model is 0.08 kg, the radius of the dead zone d_{min} is 0.003 m, the effective range of the restoring force d_{max} is 0.01 m, f_{max} in Fig. 5 is 50 N, and the coefficients in (1) and (2), k and c, are set to $f_{max}/(d_{max}-d_{min})$ and 100 Ns/m respectively.

Since an actual restoring force of a weed is intricate, it is impossible to express the actual restoring force completely in a mathematical way. Hence, as a feasible way, the simple restoring force model in (1) and (2) was adopted in the simulations described in this paper.

III. CONTROL SCHEME

In this section, the ways of oscillating the weeding manipulator to generate a force by exploiting its oscillatory motion are discussed. Simulations conducted to justify the exploitation are shown in the next section.

Fig. 6 shows the flowchart of the control scheme adopted in this study. The manipulator following this scheme becomes an oscillatory state, and thereby it can generate a large force efficiently. As shown in the flowchart, the control scheme first calculates the tip position to make an oscillatory motion of the manipulator for weeding. As elaborated later in this section, two methods to calculate the desired tip position are used in the simulations.

After the calculation of the desired tip position, the desired joint angles are derived using the inverse kinematics equations shown in (3) and (4). When the joints of the manipulator become the desired joint angles, the tip of the manipulator could reach the desired tip position. The subscript d in the equations means desired, e.g. q_{1d} is the desired joint angle of the first joint. If the desired tip position is out of a reachable region of the manipulator, the previous desired joint angles are used as the current desired joint angles.

$$q_{1d} = \cos^{-1}\left(\frac{x_{t2d}^2 + y_{t2d}^2 + l_1^2 - l_2^2}{2l_1\sqrt{x_{t2d}^2 + y_{t2d}^2}} \right) + \tan^{-1}\left(\frac{y_{t2d}}{x_{t2d}} \right) \quad (3)$$

$$q_{2d} = -\cos^{-1}\left(\frac{x_{t2d}^2 + y_{t2d}^2 - l_1^2 - l_2^2}{2l_1 l_2} \right) \quad (4)$$

Finally, as shown in the flowchart, the torques driving the joints to achieve the desired joint angles is calculated by the following simple control algorithm. The proportional gain K_p is set to 100.

$$\tau_1 = K_P(q_{1d} - q_1) \quad (5)$$
$$\tau_2 = K_P(q_{2d} - q_2) \quad (6)$$

As stated before, two methods calculating the tip position of the manipulator are used in the simulations shown in this paper. One of the methods uses a sinusoidal wave function to determine the desired tip position of the manipulator. The other uses a nonlinear oscillator which is called Van der Pol (VDP) oscillator. The two methods are elaborated in the following subsections.

A. Method using Sinusoidal Wave Function

In the method discussed in this subsection, the desired tip position is determined using a sinusoidal wave function. The following equations explain the method.
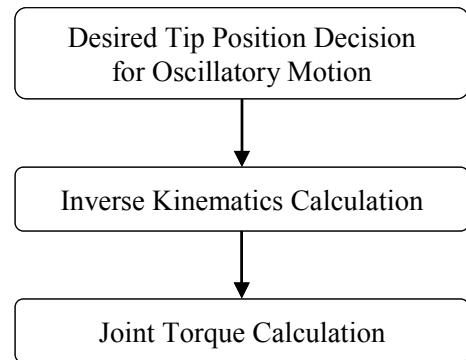

Fig. 6 Flowchart of Control Scheme.

$$x_{t2d}(t) = x_{t2}(0) - a_x \cdot t \qquad (7)$$

$$y_{t2d}(t) = \begin{cases} y_{t2}(0) & (t < t_{osc}) \\ y_{t2}(0) + a_y \cdot (t - t_{osc}) \cdot \sin(2\pi f_{osc}t) & (t \geq t_{osc}) \end{cases}$$
$$(8)$$

In the equations, t_{osc} is a time to start oscillating the manipulator that is set to one second here. The f_{osc} represents the frequency of the oscillation. The a_x and a_y are constant parameters that are set to 0.005 and 0.05 respectively. As explained in the equations, during the first one second, the manipulator only draws the weed toward its base along the x-axis, without oscillation. Then the oscillation of the tip of the manipulator along the y-axis is started to pull the weed out efficiently.

B. Method using Van der Pol Oscillator

The method discussed in this subsection uses the VDP oscillator, to which the state of the manipulator in oscillatory motion is given. Based on the state of the VDP oscillator, the desired tip position for force generation is determined. Since the VDP oscillator has a frequency entrainment property [9], the desired tip position determined by this method could synchronize with the motion of the manipulator. This adjustability would achieve the better performance than the method using a sinusoidal wave function.

This method using the VDP oscillator is expressed by the following equations.

$$x_{t2d}(t) = x_{t2}(0) - a_x \cdot t \qquad (9)$$

$$y_{t2d}(t) = \begin{cases} y_{t2}(0) & (t < t_{osc}) \\ y_{t2}(0) + a_y \cdot (t - t_{osc}) \cdot \dot{x}_v(t) & (t \geq t_{osc}) \end{cases} \qquad (10)$$

$$\ddot{x}_v + \varepsilon(x_v^2 - 1)\dot{x}_v + \omega_v^2 x_v = G_{in}\dot{y}_{t2} \qquad (11)$$

As shown in (9), the tip motion along the x-axis is same to the method using a sinusoidal wave function. With respect to the y-axis motion, the desired tip position is calculated using the state of the VDP oscillator as shown in (10). The differential equation in (11) expresses the dynamics of the VDP oscillator, where x_v is its state, ε is a positive parameter controlling the damping term, f_v is its natural frequency, $\omega_v = 2\pi f_v$. These parameters are set as follow: $\varepsilon = 1.0, f_v = 0.5$ Hz.

A self-induced oscillation of the VDP oscillator at the natural frequency occurs when it has no input signal. Fig. 7 shows the self-induced oscillation, the vertical axis represents dx_v/dt. The initial state of the VDP oscillator is set to $x_v = 1.0$, $dx_v/dt = 0.0$.

As shown in (11), the tip velocity of the manipulator along the y-axis dy_{t2}/dt is inputted into the VDP oscillator through the gain G_{in}. The gain G_{in} should be high so that the VDP oscillator can entrain to the motion of the manipulator. Using the derivative of the x_v and y_{t2} in this method has the effect of removing any DC components from these signals [10].
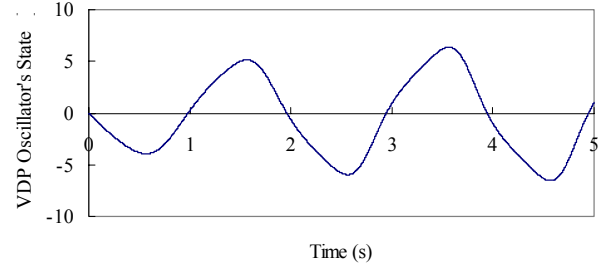

Fig. 7 Self-induced oscillation of the VDP oscillator. The natural frequency of the oscillator is set to 0.5 Hz.

IV. SIMULATION RESULTS

Simulations were conducted to appraise the effectiveness of force generation by the manipulator exploiting its oscillatory motion, using the manipulator model and the weed model created by the ODE shown in Fig. 3. In the ODE simulations, the time step size for numeric integration was set to 0.001s. The simulation results are shown in this section. To begin with, let me describe a simulation in which the manipulator keeps only drawing the weed toward its base; in this case the manipulator does not exploit its oscillatory motion. Then the simulation results that show the behaviors of the manipulator driven by one of the methods exploiting its oscillatory motions are shown. By comparing these simulation results, the effectiveness of the method discussed in the previous section is appraised.

Fig. 8 shows the force generated by the manipulator only drawing the weed without an oscillatory motion. In this case, the weeding manipulator failed to pull the weed out because the generated force was approximately 25.8 N, which is small for pulling out the weed model.

Fig. 9 shows the force generated by the manipulator driven by the method using a sinusoidal wave function, and Fig. 10 shows the displacement of the weed. The frequency of the sinusoidal wave function was set to 3.8 Hz.

As shown in Fig. 10, the weed was moved from the base point more than 0.01 m, which is the radius of the effective range of the restoring force d_{max}. Accordingly the manipulator succeeded in weeding.

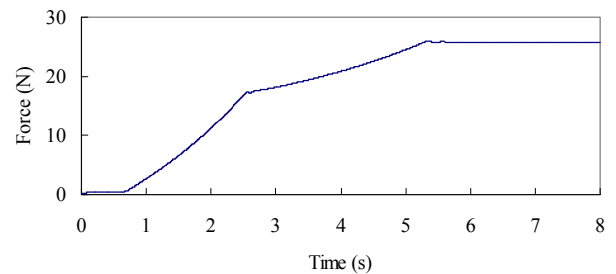Elapsed times for weeding are plotted in Fig. 11. If the

Fig. 8 Force generated by the manipulator not exploiting its oscillatory motion. The manipulator only drew the weed without oscillatory motion.

manipulator could not pull the weed out within five seconds, the simulation was aborted. The horizontal axis indicates the frequency of the sinusoidal wave used in the method. Based on the results shown in this plot, the frequency was set to 3.8 Hz in the simulation shown in Fig. 9 and Fig. 10. As the frequency was 3.8 Hz, the elapsed time for weeding was the shortest.

Fig. 12 shows the torques applied to the joints of the weeding manipulator to pull the weed out, they were calculated using (5) and (6). Although the joint torque was limited to 1.0 Nm, the manipulator exploiting its oscillatory motion was able to generate more than 70 N, which is impossible for the manipulator only drawing the weed without an oscillatory motion. However, as shown in Fig. 12, the applied joint torques vibrated at high frequency, which is a phenomenon that should be avoided if possible because it requires a high-performance motor drive system. This is a
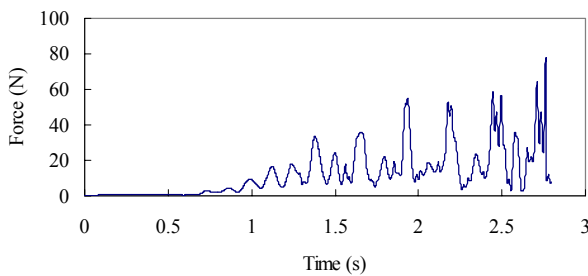

Fig. 9 Force generated by the manipulator driven by the method using a sinusoidal wave function. The frequency of the sinusoidal wave is 3.8 Hz.
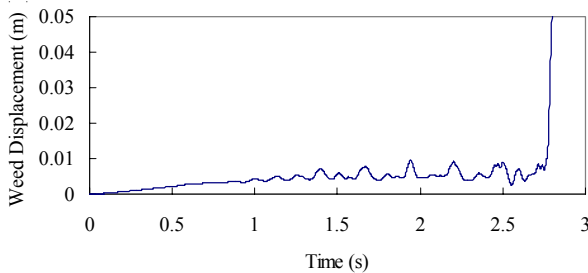

Fig. 10 Displacement of the weed pulled by the manipulator driven by the method using a sinusoidal wave function. The manipulator succeeded in weeding.
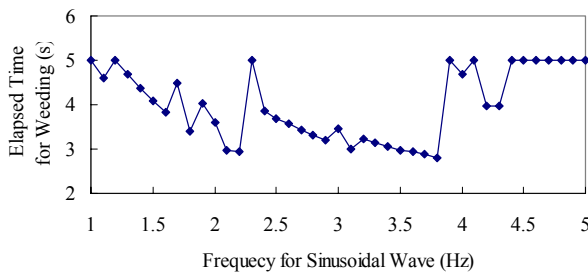

Fig. 11 Elapsed times for weeding. The manipulator was driven by the method using a sinusoidal wave function. The horizontal axis indicates the frequency of the sinusoidal wave.

defect of the method using a sinusoidal wave function.

The method using the VDP oscillator was devised in hopes of removing the defect by the entrainment property of the oscillator. Fig. 13 shows the force generated by the manipulator driven by the method using the VDP oscillator. The gain G_{in} was set to 2000 so that the entrainment could happen certainly.

As with the manipulator driven by the method using a sinusoidal wave function, the manipulator driven by the method using the VDP oscillator succeeded in weeding. Moreover, the elapsed time for weeding was reduced by about one second; the result indicates that the VDP oscillator enhanced efficiency in weeding. Fig. 14 shows the state of the VDP oscillator and the tip velocity along the y-axis of the manipulator. Thanks to the entrainment property of the VDP oscillator, its state almost synchronized with the tip motion of the manipulator. Since the desired tip position of the manipulator was calculated from the synchronized state, the efficient force generation could be achieved. In the method, it would appear that the VDP oscillator works to appropriately oscillate the manipulator based on the state of the manipulator in order to realize the efficient force generation. As shown in Fig. 15, however, the joint torques remained vibrating at high frequency.

To solve the problem, the gain G_{in} was decreased to 500 in the simulation shown in Fig. 16 and Fig. 17. Although this gain decrease caused the increase of the elapsed time for weeding, the vibration of the joint torque could be reduced. The trade-off between the elapsed time and the vibrating joint torque depends on the gain G_{in} tuning.
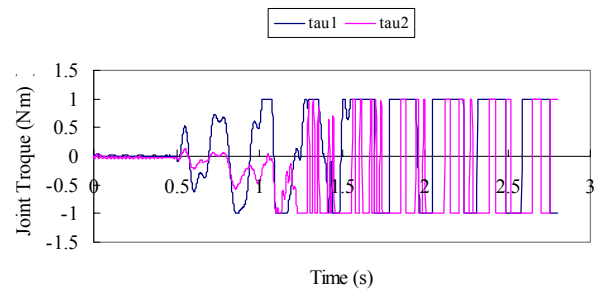

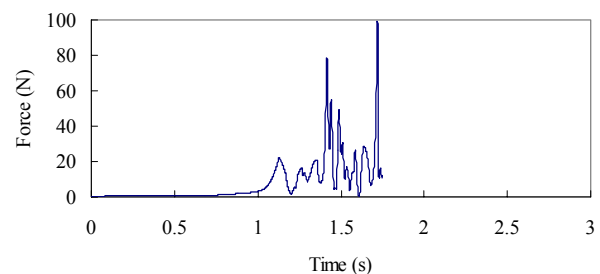Fig. 12 Joint torques applied to the weeding manipulator during the simulation shown in Fig. 9 and Fig. 10.

Fig. 13 Force generated by the manipulator driven by the method using the VDP oscillator. The gain G_{in} is 2000.
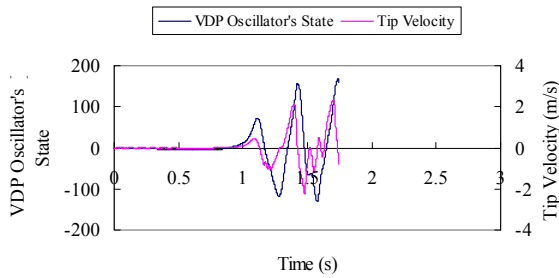
Fig. 14 VDP oscillator's state dx_v/dt and the tip velocity of the manipulator dy_{t2}/dt. The VDP oscillator's state almost synchronized with the tip velocity. The gain G_{in} is 2000.
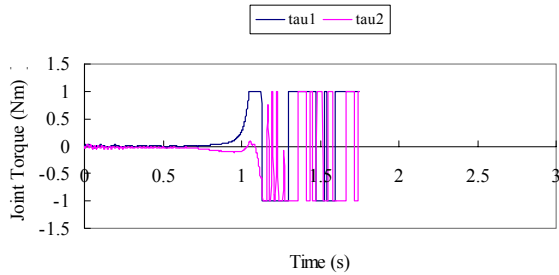

Fig. 15 Joint torques applied to the weeding manipulator during the simulation shown in Fig. 13 and Fig. 14.
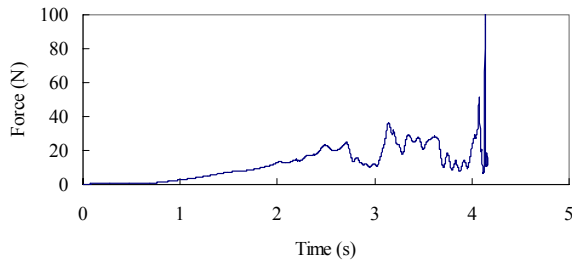

Fig. 16 Force generated by the manipulator driven by the method using the VDP oscillator. The gain G_{in} is 500.
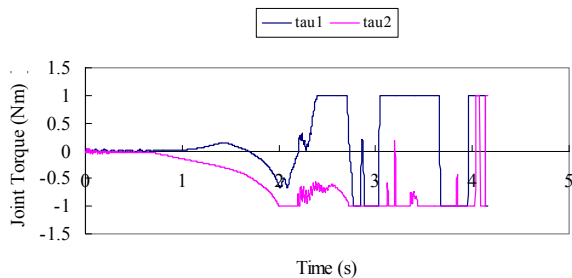

Fig. 17 Joint torques applied to the weeding manipulator during the simulation shown in Fig. 16.

III. CONCLUSIONS

To justify the exploitation of an oscillatory motion of the weeding manipulator for efficient force generation, some simulations were conducted based on the manipulator model and the weed model created using the ODE that was used to

make more practical situation in the simulations. According to the simulation results, a large force that the manipulator not exploiting its oscillatory motion could not generate was achieved by the manipulator driven by the methods introduced in this paper. Moreover, it was demonstrated that the method using the VDP oscillator could realize better force generation than the method using a sinusoidal wave function, because of the entrainment property of the VDP oscillator. Experiments that make the method for force generation more convincing will be carried out using a manipulator with adjustable joint stiffness being assembled in the author's lab.

REFERENCES

[1] E. Papadopoulos and Y. Gonthier, "A Framework for Large-Force Task Planning of Mobile and Redundant Manipulators," *Journal of Robotic Systems*, vol. 16, no. 3, pp. 151-162, 1999.

[2] J. Imamura and K. Kosuge, "Handling of an Object Exceeding Load Capacity of Dual Manipulators Using Virtually Unactuated Joints," in *Proceedings of the 2002 IEEE International Conference on Robotics & Automation*, pp. 989-994, 2002.

[3] J. Kobayashi, S. Kishida, and F. Ohkawa, "Analysis of Suitable Postures for Robot Manipulator Applying Force using Numerical Optimization Method," in *Proceedings of International IEEE Conference Mechatronics & Robotics 2004*, Part II, pp. 277-282, 2004.

[4] J. Kobayashi and F. Ohkawa, "Efficient Oscillation Method with Nonlinear Oscillator for Large Force Generation of Manipulator Exploiting Oscillatory Motion," in *Proceedings of the 2006 IEEE International Conference on Robotics and Biomimetics*, pp. 351-356, 2006.

[5] J. Kobayashi and F. Ohkawa, "Force Control System with Nonlinear Oscillator for Manipulator in Oscillatory Motion," in *Proceedings of the 2007 IEEE International Conference on Robotics and Biomimetics*, pp. 2166-2171, 2007.

[6] Open Dynamics Engine, http://www.ode.org/.

[7] G. A. Pratt and M. M. Williamson, "Series Elastic Actuators," in *Proceedings of the IEEE/RSJ International Conference on Intelligent Robots and Systems*, vol. 1, pp. 399-406, 1995.

[8] B. Bill and I. R. Harvey, "Programmable springs: Developing actuators with programmable compliance for autonomous robots," *Robotics and Autonomous Systems*, vol. 55, pp. 728-734, 2007.

[9] D. W. Jordan and P. Smith, *Nonlinear Ordinary Differential Equations: An Introduction to Dynamical Systems (Third Edition)*, Oxford University Press, pp. 253-257, 1999.

[10] P. Veskos and Y. Demiris, "Development acquisition of entrainment skills in robot swinging using van der Pol oscillators," in *Proceedings of the EPIROB-2005*, pp. 87-93, 2005.